DOKUZ EYLÜL UNIVERSITY

GRADUATE SCHOOL OF NATURAL AND APPLIED SCIENCES

A STUDY ON THERMOPHYSICAL PROPERTIES OF GRAPHITE FILLED POLYMER NANOCOMPOSITES

by

Berkan EMEK

February, 2013

İZMİR

A STUDY ON THERMOPHYSICAL PROPERTIES OF GRAPHITE FILLED POLYMER NANOCOMPOSITES

A Thesis Submitted to the
Graduate School of Natural and Applied Science of Dokuz Eylül University In Partial Fulfillment of the Requirements for the Degree of Master Science in Mechanical Engineering, Energy Program

by
Berkan EMEK

February, 2013
İZMİR

M.Sc THESIS EXAMINATION RESULT FORM

We have read the thesis entitled **"A STUDY ON THERMOPHYSICAL PROPERTIES OF GRAPHITE FILLED POLYMER NANOCOMPOSITES"** completed by **BERKAN EMEK** under supervision of **PROF. DR. İSMAİL HAKKI TAVMAN** and we certify that in our opinion it is fully adequate, in scope and in quality, as a thesis for the degree of Master of Science.

Prof. Dr. İsmail Hakkı TAVMAN

Supervisor

Yrd. Doç Dr. Mehmet SARIKANAT

(Jury Member)

Yrd. Doç. Dr. Alpaslan TURGUT

(Jury Member)

Prof.Dr. Mustafa SABUNCU

Director

Graduate School of Natural and Applied Sciences

A STUDY ON THERMOPHYSICAL PROPERTIES OF GRAPHITE FILLED POLYMER NANOCOMPOSITES

ABSTRACT

In this work, graphite powder (30 nm) which has heat capacity was mixed with HDPE in the Brabender Plasticorder mixer in certain conditions. Nanocomposites containing (4, 6, 8, 10, 12, 15, 17, 20, 22 percent) weight fractions of graphite were fabricated. Heat capacity of high-density polyethylene (HDPE)-graphite nanocomposites is investigated experimentally and the results are compared with the theoretical model. Differential scanning calorimetry is used to measure the heat capacity of nanocomposites consisting different weight fractions of high-density polyethylene (HDPE) matrix filled with graphite.

Keywords: Polymer nanocomposite, heat capacity, HDPE, graphite, DSC

GRAFİT KATKILI POLİMER NANOKOMPOZİTLERİN TERMOFİZİKSEL ÖZELLİKLERİ ÜZERİNE BİR ÇALIŞMA

ÖZ

Bu çalışmada, yüksek ısıl iletkenlik değerine sahip grafit tozu (30 nm) ile yüksek yoğunluklu polietilen (YYPE) Brabender Plasticorder cihazında belirli koşullar altında karıştırılmış ve yüzde (4, 6, 8, 10, 12, 15, 17, 20, 22) kütlesel katkı oranlarında nanokompozitler üretilmiştir. YYPE-grafit nanokompozitin ısı kapasitesi deneysel olarak araştırılmış ve teorik modelle karşılaştırılmıştır. Farklı kütlesel katkı oranlarındaki yüksek yoğunluklu polietilen (YYPE)-grafit nanokompozitin ısı kapasitesi DSC cihazıyla ölçülmüştür.

Anahtar sözcükler: Polimer Nanokompozit, ısı kapasitesi, YYPE, grafit, DSC

CONTENTS

Page

CHAPTER ONE

INTRODUCTION

In recent years , with increasing development in technology , instead of the usual metal and metal alloys, composite materials with various structures have been used. This composite materials come into our lives with each passing day and they play a very important role in numerous fields of everyday life (electronics, textile, health, aeronautics, transportation etc.) due to their advantages over conventional materials such as lightness, resistance to corrosion, ease of processing and low cost production. As a result of this, composite materials, especially nanocomposite materials, are becoming increasingly important in industry and most of the researchers show great interest in these composites.

1.1 Composites

Composite materials, obtained by distribution of at least two materials with different structures and properties in a microscopic scale homogeneously within one another, are defined as materials with new properties. Polymer, metal and ceramic composites are the main constituents. Polymers have the characteristic of low density, high chemical resistance, easy formability. However, the poor mechanical and thermal endurance limits the application areas. Ceramics have a low density like polymers , but they are the biggest disadvantages of hard and brittle, therefore this materials are difficult to be shaped.

The classification of composite materials according to the type of matrix is divided into three:

1- Polymer Composites

2- Metal Composites

3- Ceramic Composites

Metallic composites are prepared with the distribution of the filler in the metallic matrix using techniques such as melting and hot pressing. Metallic composites are generally use in aerospace and aviation industries. For instance, platform carrier parts, space communications equipment etc.

Ceramic composites are obtained with the use of several compounds which are metal or non-metal (Al2O3, SiC, B4C, CbN, TiC, Si3N4, etc.). Ceramic composites are used in the manufacturing of the spacecraft parts, electrical, medical materials, and parts for military purpose.

Polymer composites are obtained by combining a natural or synthetic filler with the polymer matrix. Polymer composites have superior features such as High-strength, dimensional and thermal stability, hardness and abrasion resistance.

1.1.1 Properties of Composite Materials

There are four main factors that determine the properties of composite materials. These properties;

1. Matrix properties
2. Reinforcing filler properties
3. Interface properties
4. Microstructure properties

Matrix component or reinforcing filled alone do not have the properties can be achieved by the preparation of composites. For this reason, it is possible to talk advantages and disadvantages of composite materials. These advantages and disadvantages are :

High strength: Tensile and flexural strength of composites is much higher than many metallic materials. In addition, thanks to their molding properties, they can be given necessary strength in the desired direction and area. Thus, cheaper products are obtained by saving material.

Easy shaping: Large and complex parts can be molded in one piece by an operation. This enables us to gain from material and labour.

Electrical Specifications: With the appropriate selection of materials, composite products which has a superior electrical properties can be produced. Today composites are used in large power transmission lines as a good conductor and if necessary, in another form, they can be used as a good conductor material.

Resistant to Corrosion and Chemical Effects: Composites are not affected by weather effects, corrosion and most chemical effects. Thanks to these properties, composite materials are safely used in chemical tanks, pipes and extractors, in the production of boats and other marine vehicles. Especially, its resistance against corrosion is advantage for many areas of industry.

Heat and Flame Resistance: Heat resistance of composites, which can be made from low thermal conductive material, makes it possible to use under high temperature. Their thermal conductivity can be increased with some special admixture material.

Permanent Coloring: Composite materials can be given desired color by adding pigments to resin during the molding process. This process does not require additional expenses or labour.

Vibration Damping: Composite materials have a natural characteristic of vibration and shock damping thanks to ductility. Fracture walking incident can be minimized by this way.

Apart from these positive characteristics, unsuitable characteristics of composite materials are as follows:

- Air particles of the composite materials has negative effect on fatigue properties of material.
- Composite materials show different properties in different directions.
- For the same composite material; tensile, compression, shear and bending strength values vary.
- Precision manufacture of this kind of material is not possible since processes like drilling, cutting holes causes fibers to open up.

As seen, composite materials, has many advantages compared to aluminum and steel despite of some disadvantages. By these features, composites are materials

which can solve many problems in many industries like from car body and bumpers to sea boats, from building facades and boards to bathroom units, from household appliances to agricultural machinery.

1.2 Polymer Nanocomposites

At least one component of the composite of the materials having a size of nanometer (10^{-9}) level, the new class of composite materials "nanocomposites" noun form. Nowadays, ceramic nanocomposite materials, polymer nanocomposite materials and metal nanocomposite materials are produced and studies on production and properties of these materials attract great interest in industry as well as to in the scientific environment.

Polymer nanocomposites ,which are distributed organic or inorganic nanoparticules in the polymer, are defined as composite materials which include natural or synthetic second phase or the filler (Durmuş,2006).

The first studies was initiated by Toyota Research Group in the 1980s. Nylon-6/clay nanocomposite ,which developed in the Toyota Research Laboratories, 50-70% relative to the polyamide (PA) and PA composite which prepared by conventional fillers was found to be superior mechanical and thermal properties. Nylon-6/clay nanocomposite first industrial use began with the production of the Toyota brand cars seat belt in 1991 (Gao,2004). Soon after, nylon-6/clay nanocomposites was used for the production of car doors, coatings for car engines, and the rear part of the car seats.

Polymer nanocomposites generally consist of two main components. These are the original material matrix-forming polymer material and nano-sized filler material. In same cases, the third component (compatibilizer) is used for to enhance the interaction between the polymer phase and fillers.

1.2.1 Polymer

Polymer matrix is the main component affecting the physical properties of the obtained nanocomposites and acts as a glue that holds together the filler.

1.2.2 Nano-Sized Filler

"Nanoparticules" are with a size of at least one nanometer (10^{-9}) level is defined as the particles. The mechanical, electrical, thermal, optical and chemical properties of the particles change when the size of the particles become smaller at the nanometric level. Therefore, the nanoparticules change the properties of structure in which they are found. The most important distinguishing property between microparticules and nanoparticules is their having a larger surface area per unit volume. As the size of the particles reduce, increasing surface area to volume ratio leads atomic behavior to be dominant on the particle surface rather than atomic behavior inside particles. This situation is changing both single-particle properties and interaction with other particles (Holister,2003).

The geometry, size, length / width ratio (aspect ratio)(Figure 1.1), distribution, surface properties, amount and type of nanoparticle that used as filler material in polymer nanocomposites parameters are directly affect the properties of nanocomposites obtained. Small size and large surface area of nano-filler, increases the interfacial interaction between the components that make up the structure. Therefore, it is possible to get the structures which have much better physical properties considering microparticules which have smaller surface area.

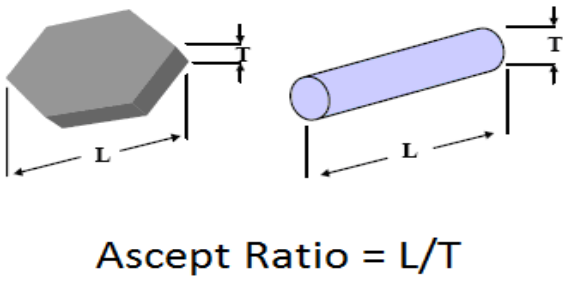

Figure 1.1 Accept Ratio

The polymer nanocomposite materials ,which have lower gas permeability in comparison with pure polymer and other composite structures, can be prepared by nano-fillers with high aspect ratio (Liang ,2004). Besides nano-fillers in the form of particle, the strength of mechanical properties and the values of the elastic modules are enabled to get better the toughness of the material (Chan, 2002).

Also, nanoparticules ,which have size below the critical wavelength of light are transparent, enable to use filler in the preparation of the materials in which transparency is essential (Holister, 2003).

The distribution of nano-filler in the polymer matrix is one of the most important parameters that affect the properties of nanocomposites obtained. The distribution of nano-filler within structure, significantly depends on the method of preparation of nanocomposites and surface modification of nano-filler (Hussasion, 2006; Tian, 2005).The change of surface features of nano-filler from the organic modification ,improving the interaction between the distribution of the nano-filler and the polymer filler, enables to obtain much better materials which are obtained by nano-filler than the materials which are obtained by nano-filler without surface modification.

1.3 Properties of Polymer Nanocomposites and Literature Review

1.3.1 Thermal Properties

Thermal property, is one of the most important characteristic of polymeric materials, is the main factor that affects the mechanical properties of the material, durability and physical life. In comparison with metal and ceramic materials, The weaker thermal properties of polymeric materials can be improved with the participation of stable, rigid, aromatic or heterocyclical structures in the chains of polymer. Thermal endurance of the polymer matrix can be increased by the addition of inorganic nano-fillers. Polymer nanocomposites compared to the pure polymers degradation and show a decrease in rate of decomposition at high temperatures (Peng,2007). This situation can be observed even in very low nano-filler content. Another important change brought about by the thermal properties of polymers with nano-fillers to delay combustion (flame retardant). Instead of a large amount of

conventional inorganic materials, used as fire retardants, resulting from the synergical interaction of nano-fillers combustion can be delayed with low quantities of these materials (Wei ,2006). The contribution of thermal properties of inorganic nano-fillers is explained by the barrier model. This layer is formed on the surface of the polymer acts as a barrier to mass and heat transfer and limits the surface migration of degradation products (Peng ,2007).

According to Tavman (1996), experimental results of HDPE/tin (Sn) composites showed that a region of low particle content, up to about 10% volume concentration, where the increase in thermal conductivity is quite slow. In this region, the filler particles are disintegrated in the matrix material. The thermal conductivity is best estimated by Maxwell's and Nielsen's models. In those models, their result was A=1.5, ϕm=0.637. However, at high filler concentrations, the filler particles incline to emerge agglomerates and conductive chains in the direction of heat flow. As a result, a rapid increase emerges in thermal conductivity. A model developed by Agari and Uno estimates the termal conductivity by means of employing two experimentally determined constants (Tavman,1996).

According to Tekce, Kumlutas and Tavman (2007), polyamide and copper (Cu) particles(fiber, spherical, prismatic) are examined. This study shows that When the concentration value of 10% is exceeded, a rapid increase emerges for the copper fiber filled polymer composite in the thermal conductivity. However, it does not emerge for the spherical or prismatic copper filled polymer composites. The rapid increase can be linked with the beginning of the interactions among the copper fibers. Because it should be underlined that the rapid increase is not the same with the other types of fillers, but same just after exceeding the 10 vol% filler concentration (Tekce et al.,2007).

In the Tlili, Boudenne, Cecen, Ibos, Krupa & Candau (2010)'s study, an increase of thermal conductivity (λ) was observed with increasing filler content for all samples investigated. This increase of λ may be foreseen due to the filler's having a notably higher thermal conductivity compared to the polymeric matrix. It is also observed that EVA/UG composites have a higher thermal conductivity in comparison with the EVA/EG ones at the same concentration. For a given

concentration, the heat propagation is influenced by the filler size and the aspect ratio in the composite (Tekce et al.,2007).

In graphite content, the thermal conductivity measurements of composites revealed their nonlinear increase with increase. The thermal conductivity of filled LDPE is lower than the thermal conductivity of filled HDPE. It stems from the higher degree of crystallinity (Kurupa et al., 2004).

Because crystalline phase (regular structure) leads a better heat transportation rather than amorphous phase, semi crystalline matrices have higher thermal conductivity and thermal diffusivity compared to amorphous matrices. At the same concentration, the composites filled with graphite KS own higher thermal conductivity than composite filled with graphite EG. In conclusion, it is assumed that both types of graphite have the same thermal conductivity and this fact leads to higher aggregation of smaller graphite KS particles (Krupa & Chodak, 2001).

1.3.1.1 Thermal Effect of Composite Fillings

1.3.1.1.1 Carbon-based fillers. Carbon-based fillers seem to be the best encouraging fillers, matching high thermal conductivity and lightweight. The most familiar conventional carbon-based fillers are graphite, carbon fiber and carbon black. Graphite has good thermal conductivity, low cost and fair dispersibility in polymer matrix. For this reason, it is generally considered as the best conductive filler (Causin et al., 2006) and (Tu & Ye, 2009).

Single grapheme sheets which forms graphite display innately high thermal conductivity of about 800 W/m K (Liu et al., 2008) or higher (theoretically estimated to be as high as 5300 W/m K (Veca et al., 2009) and (Stankovich et al., 2006). The high thermal conductivity of graphite is generally reported between 100 to 400 W/m K.

Expanded graphite (EG) is a form of graphite which is separated into layers of 20-100 nm thickness. It has also been employed in polymer composites (Ganguli et al., 2008), for which the thermal conductivity depends on the exfoliation degree (Park et al., 2008).

Carbon fiber is another essential carbon-based filler which is generally employed as vapor grown carbon fiber (VGCF). (Tibbetts et al., 2007).

Because VGCF is comprised of a ring-shaped geometry parallel to fiber axis, thermal conductive properties along the fiber axis are very divergent from the transverse direction (estimated up to 2000 W/m K in the axial direction vs. 10–110 W/m K in the transverse direction (Chen & Ting, 2002) and (Zhang et al, 2000)), directly affecting the thermal conductivity of aligned composites (Mohammed & Uttandaraman, 2009) and (Kuriger et al., 2002).

Piles of graphite microcrystals and characteristic of their particle size (10–500 nm) and surface area (25–150 m2/g) emerge carbon black particles (Pierson, 1993). Carbon black makes much more contribution to electrical conductivity rather than thermal conductivity. (Wong et al., 2001), (Abdel-Aal et al., 2008) and (King et al., 2006).

1.3.1.1.2 Metallic fillers. The filling of a polymer with metallic particles may be concluded with both increase of thermal conductivity and electrical conductivity in composites. However, a density increase is also obtained when adding significant metal loadings to the polymer matrix, thus limiting applications when lightweight is required. Powders of aluminium, silver, copper and nickel contain in metallic particles which are employed for thermal conductivity improvement. Boudenne et al studied the thermal behavior of polypropylene filled with copper particles (Kumlutaş et al., 2003).

In a good estimation, the thermal conductivity of composites is provided by Agari's model. Polymers, which are changed with the inclusion of metallic particles include polyethylene (Kumlutaş et al., 2003), polypropylene (Boudenne et al., 2005), polyamide (Tekce et al., 2007), polyvinylchloride and epoxy resins (Mamunya et al., 2002), present thermal conductivity performance based on the thermal conductivity of the metallic fillers, the particle shape and size, the volume fraction and spatial arrangement in the polymer matrix.

By using the laser flash method, thermal conductivity of a powder injection molding feedstock (mixture of metal powders and polymers) in solid and molten

states has been measured. An attempt has been made to employ two most promising existing mathematical models (theoretical Maxwell- and semi-theoretical Lewis & Nielsen model) to calculate the thermal conductivity of the mixture. At the end of the attempt, it is calculated that the Lewis & Nielsen model predicts better than Maxwell model the thermal conductivity of the feedstock. As the difference between the calculated (Maxwell model) and the measured results amounts to 15–85%, it is suggested that it can only be used for preliminary assessment of the thermal conductivity of so highly filled composite material. If accurate thermal conductivity data are required (as in case of numerical simulation of the powder injection moulding process), measurement of this property has to be performed if meaningful simulation results are to be expected (Ebadi, Nazempour., 2012).

1.3.1.1.3 Ceramic fillers. Ceramic powder which strengthens polymer materials, has been used extensively as electronic materials. Many ceramic materials, for instance, aluminum nitride (AlN), boron nitride (BN), silicon carbide (SiC) and beryllium oxide (BeO) become more of an issue as thermally conductive fillers because of their high thermal conductivity and electrical resistivity (Nu et al., 2008) and (Ishida & Rimdusit, 1998).

Thermal conductivities of composites with ceramic filler are affected by filler packing density (Ohashi et al., 2005), particle size and size distribution (Yu et al., 2002) and (Mu et al., 2007), surface treatment (Gu et al., 2009) and mixing methods (Zhou et al., 2007).

The thermal conductivity of polymer composites are disputed in terms of the models and theories. Effective Medium Theory (EMT), Agari model and Nielsen model are respectively presented and applied as assumptions for the thermal conductivity of ceramic particle.

In conclusion: both EMT and Nielsen model may present a good prediction for the thermal conductivity at a low volume fraction of the filler; if it is considered as a whole, it could be said that Agari model presents a better prediction despite its larger error percentage (He et al., 2007).

Tablo 1.1 Thermal conductivities of some thermally conductive fillers (Ebadi & Nazempour,2012)

Material	Thermal Conductivity at 25 °C (W/m K)
Graphite	100~400 (on plane)
Carbon black	6~174
Carbon Nanotubes	2000~6000
Diamond	2000
PAN-based Carbon Fibre	8~70 (along the axis)
Pitch-based Carbon Fibre	530~1100 (along the axis)
Copper	483
Silver	450
Gold	345
Aluminum	204
Nickel	158
Boron Nitride	250~300
Aluminum nitride	200
Beryllium oxide	260
Aluminum oxide	20~29

1.3.2 Melting Properties

Knowledge of the melting properties of polymeric materials allows the acquisition of information about the workability of the material. Melting properties directly affected by the amount and properties of the components. Melting properties are determined by mixing torque-time curves that are generally obtained in studies torque rheometer. Specific points of this curve can be determined , melting temperature , melt down period , melting energy , melting torque.

Nano-fillers influence on the melting properties of polymer matrix depends on the amount of filler and surface modification. Generally, nano-fillers need fewer melting time, temperature and higher melting torque in comparison with micro size fillers. This condition puts into practice regarding to surface area of fillers, friction forces created and contributions of thermal conduction.

1.3.3 Mechanical Properties

As a result of blending of inorganic filler material with 1-10% by weight polymer matrix, mechanical properties can be improved. This rate is between 20-50% by weight for micro-sized fillers (Qian, 2004). Since inorganic fillers have a higher density than polymers, density of filled polymers is higher than pure polymers. Compared to other materials, one of the biggest advantages is light weight thanks to low density, since use of it with filler material will worsen, it is desired to use the least possible amount of filler (Hasan, 2006). While excessive use of rigid structured filler materials results as hardness of polymer composite, it causes reduction of flexibility and impairment of processability (Xiong, 2005). In the case of polymer nanocomposites, effect of these disadvantages remains minimum and in some cases even improvements can be achieved.

Strength and toughness are the most important mechanical characteristics of the material. Nanoparticles structured with layer and fiber can provide significant improvements in strength and modulus values thanks to their high length / width ratio. However, toughness of nanocomposites prepared with this kind nanoparticles that has the high length / width ratio cannot be increased and sometimes it decreases (Cho, 2001). This situation for particle-structured nanoparticles is different. The spherical nano-fillers, which has length / width ratio close to one, large surface area and high surface energy, provides better toughness with strength and modulus thanks to a strong interfacial interaction between filler and polymer matrix. (Sun, 2006; Chen, 2004)

The mechanical properties of composites, which contains micro-sized filler material, only depend on the volume fractions of the components and their own mechanical characteristics. However, it is considered that network structure formed between nanoparticles are other effects improving the mechanical characteristics of polymer matrix along with volume fraction of filler as a result with the decrease of size of filler material in constant volume fraction of nanocomposites and decrease in the distance between the adjacent surfaces of nanoparticles with shrinking of diameter of the nanoparticles and overgrowth of polymer filler interface. (Ozmusul, 2006).

Nanoparticle size and surface properties and distribution along with method of preparation of nanocomposite are among the parameters affecting the mechanical properties of nanocomposites. It is reported that prepared by the method of simultaneous polymerization of poly (dimethyl siloxane) - silica nanocomposite's strength is higher than strength of nanocomposites prepared with the other methods due to a better distribution of nano filler with this method (Sun, 1989). It is reported that as a result of decrease in particle-particle interaction surface energy due to nanoparticle surface modification, agglomeration of nanoparticules are prevented and it contributes to homogeneous distribution. Thanks to these, mechanical properties are improved. (Zuiderduin, 2003). It is established that module values of composites prepared by micron-sized filler materials are affected but with the decrease of size of the nano-filler, module values of nanocomposites increase. It is established that tensile strength increases with decreasing particle size but as a result of the lack of good distribution of nanoparticles in nanocomposites which has high ratio nano-sized filler, tensile strength compared with composites containing micro-sized filler is much lower (Cho, 2006).

HDPE-graphite mixtures in different weight percentage (wt.%) were prepared in a Brabender Plasticorder PLE 331 internal mixer. In conclusion, the resulting nanocomposite properties were compared with those of graphite in different weight percentage (wt.%) filled HDPE composite. When 6 wt.% expanded graphite in HDPE was loaded, the maximum tensile strength and the modulus upgraded over the neat HDPE film by about 53 and 46% sequentially. The modulus of HDPE increases with increasing graphite content from 8% to 30%. However, at a higher loading of 8 wt.%, the tensile strength exhibited significant decrement (Sarıkanat et al.,2011).

The stiffness of the HDPE-54 + 2%, 4%, and 8% increases by 15%, 25%, and 46% respectively when compared with HDPE-54. Because of the incorporation of the carbon nano-particles, this increase in the viscoelastic modulus was attributed to the stiffness increase of the matrix. According to the tensile tests results, it can be concluded that the HDPE nano-composites, excluding 8%, demonstrated typical cold drawing behavior before the final break of the samples. Adding the nano-particles up to 4% was not significantly influenced the elongation at the break of the nano-

composites. Moreover, it could be reported that an inconsiderable increase emerges in the tensile strength at break for the nano-composites compared with pure HDPE (Founad et al.,2011).

From this figure it may be assumed that the elongation at break decreases more rapidly when compared with the prediction from the Nielsen model up to 20% Al content. The elongation at break is virtually consistent between 20% and 45% of A1 content. For low-volume fraction of aluminum particles (up to about 12%), Einstein's equation assumption perfect adhesion between the particles and polymer- is relatively parallel to the experimental results. The bond among the filler particles is not as strong as that between the matrix and the particles. It should be noted that there may be spaces forming with the application of a tensile load (Tavman , 1996).

On both of the investigated systems, in graphite content, the prominent decrease of elongation at break –herewith an increase- were seen. This decrease is much more prominent than an expected decrease in Nielsen's model. Very irregular shape of particles of their graphite with many sharp edges (potential stress concentrators) is more likely responsible for this behavior (Krupa et al.,2004).

Compared with filler content, the nonlinear behavior was detected for the dependency stress at break. On the one hand, the presence of a filler ends up with an easier initiation of crack formation through stress concentration on the filler surface. On the other hand, it ends up in a decrease of chain mobility as a result of polymer-filler interactions resulting in lower deformability of the material. Hence, so long as the concentration of the filler is low, the first effect becomes more essential and prominent decrease of stress at break is detectable. If concentration of the filler increases, reinforcing effect and stress at break increases (Krupa et al.,2004).

Reinforcing effect of the both fillers affects the mechanical properties. As it is expressed in Young's modulus by increase and in the elongation at break data in decrease, the extent depends on the filler surface area (Krupa & Chodak ,2001).

1.3.4 Rheological Properties

Detailed knowledge of the rheological properties of molten polymer nanocomposites is very important in the aspect of foreseeing of processability of polymer nanocomposites. Given the fact that the success of polymer nanocomposites in application is directly related with process (Pryamitsyn, 2006; Ray, 2003), detailed knowledge of the flow behaviors is very important in the aspect of processability along with in terms of understanding the structure-property relationship. Polymer nanocomposites' molten rheology is closely linked to structure and distribution of nano filler, the interaction between particles of nano filler or between the filler and polymer matrix (Ray, 2006; Lim, 2001). It is foreseen that nanoparticles are effecting rheological properties by aggregating and creating network in studies of literature (Knauert, 2007). Nanocomposites with low rates of nano-filler showing behavior of shear thinning, having very high viscosity values in low cutting speeds are interpreted as an indication of the formation of the network structure. It is pointed out that this network structure formation does not require a physical bond formation between particles and interaction between particles depends on the length / width ratio and distance between the particles and these affect the network formation. Decrease of distance between particles in constant volume fraction or increase of the length / width ratio increases the likelihood of possibility of interaction between particles (Vlasveld, 2005). It is stated that nanocomposite molten viscosity increases due to nano-sized filler having larger surface and so it increases the interaction of polymerparticule (Zuiderduin, 2003).

1.3.5 Barrier Properties

It is established that nano fillers, especially layer structured nano fillers reduces efficiently liquid and the gas permeability of the polymer matrix. It is considered that as a result of layers with high Length / width ratio creating exfoliated form in polymer matrix, permeability decreases and this is caused by layers forming tortuous path. It is explained that layers form am impaired structure in diffusion of gas or liquid and as a result of that, with elongation of pathways permeability changes. It is

observed in studies that with the increase of length / width ratio, permeability decreases. In figure 1.2, formation of tortuous path and its comparison are shown. (Ray, 2003; Giannelis, 1996).

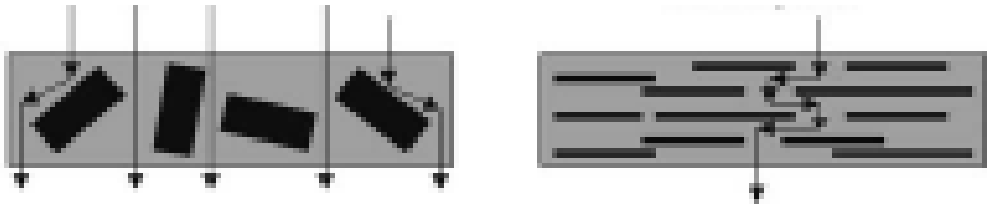

Figure 1.2 The formation of detour

1.3.6 Other Properties

Depending on the electrical properties of nano-fillers, they can be classified in two groups: conductive and non-conductive nano-fillers. Carbon nanotube, carbon black, metals and metal compounds can be given as an example to nano fillers which shows electrical conductivity and increases electrical conductivity of the polymer matrix (Du, 2004; Knite, 2004; Chen, 2001). Nano-fillers such as layered silicate, silica (SiO2), titanium dioxide (TiO2), alumina (Al2O3) are nano-fillers which can achieve improvement in the properties of the dielectric of nanocomposites (Tanaka, 2005; Roy, 2005; Magaraphan, 2001).

Size of nanoparticules which is less under the wavelength of visible light enables the production of transparent nanocomposite. Optical properties of nanocomposites can be protected in this way and they are very important in especially packaging, cosmetics and coating industries for the use of nanocomposite (Holister, 2003; Leodidou, 1996).

The crystallinity degree of polyethylene matrix does not have significant influence upon either the percolation concentration or electrical conductivity of composites. DSC measurement denotes that the filler does not play an important role on the change of the crystallinity degree of polyethylene matrices (Krupa et al., 2004).

Electrical conductivity measurements indicated that different types of graphite affect the percolation concentration of composites variously (Krupa & Chodak ,2001).

CHAPTER TWO

HEAT CAPACITI MODELS

Two things must be clarified for any theory used to calculate lattice vibration heat capacities of crystalline solids:

First of all, the well-known Dulong and Petit law: Near room temperature, the heat capacity of most solids is around 3k per atom (the molar heat capacity for a solid consisting of n-atom molecules is ~3nR).

At low temperatures, C_v decreases, becoming zero at T=0. Heat capacities have a temperature dependence of the form $\alpha T^3 + \gamma T$, where the T^3 term arises from lattice vibrations, and the linear term from conduction electrons.

Classical mechanics would predict C_v = 3R at all temperatures, in violation of both experiment and the third law of thermodynamics.

2.1 Einstein's Theory of Heat Capacities

The atoms are treated by Einstein in a crystal as N simple harmonic oscillators, all having the same frequency ν_E. The frequency ν_E depends on the strength of the restoring force having effect on the atom, i.e. the strength of the chemical bonds within the solid. Since the equation of motion for each atom decomposes into three independent equations for the x, y and z components of displacement, and Natom solid is equivalent to 3N harmonic oscillators, each vibrating independently at frequency ν_E.

The energy levels of the harmonic oscillators are given by

$$\varepsilon_\nu = h\nu_E\left(\mathrm{v} + \frac{1}{2}\right), \qquad \mathrm{v} = 0,1,2.... \tag{2.1}$$

Assuming the oscillators are in thermal equilibrium at temperature T, the partition function for a single oscillator is

$$q = \sum_{v=0}^{\infty} \exp[-\beta\varepsilon_v] = \sum_{v=0}^{\infty} \exp[-\beta h\nu_E\,(v+\tfrac{1}{2})] = e^{-x/2}\sum_{v=0}^{\infty} e^{-xv} = \frac{e^{-x/2}}{1-e^{-x}} \quad (2.2)$$

wher e $x = \beta h\nu_E$

In the above, we have used the fact that $\sum_{v=0}^{\infty} x^n = \frac{1}{1-x}$

The mean energy per oscillator is then

$$u = -\frac{d\,lnq}{d\beta} = \frac{d}{d\beta}\left[\frac{\beta h\nu_E}{2} + \ln\left(1-e^{-\beta h\nu_E}\right)\right] = \frac{h\nu_E}{2} + \frac{h\nu}{e^{-\beta h\nu_E}-1} \quad (2.3)$$

The first term above, hν/2, is simply the zero point energy. Using the fact that energy is an extensive property, the energy of the 3N oscillators in the N-atom solid is ;

$$U = 3Nu = 3N\left(\frac{h\nu_E}{2} + \frac{h\nu}{e^{-\beta h\nu_E}-1}\right) \quad (2.4)$$

The heat capacity at constant volume is thus

$$C_V = \left(\frac{\partial U}{\partial T}\right)_V = 3N\left(\frac{\partial U}{\partial \beta}\right)_V\left(\frac{\partial \beta}{\partial T}\right) = 3Nk\frac{x^2e^x}{(e^x-1)^2}] \qquad \text{where} \quad x = \frac{h\nu_E}{kT} = \frac{\theta_E}{T} \quad (2.5)$$

θ_E is the 'Einstein temperature, which is different for each solid, and reflects the rigidity of the lattice.

At the high temperature limit, when T >>θ_E (and x << 1), the Einstein heat capacity reduces to $C_V = 3Nk$, the Dulong and Petit law (prove by setting e^x~ 1+x in the denominator).

At the low temperature limit, when T << θE (and x >> 1), $C_V \to 0$ 0 as $T \to 0$, as required by the third law of thermodynamics. (Prove by setting e^x- 1 ~ e^x in the denominator for large x).

2.2 Debye's Theory of Heat Capacities

Debye improved on Einstein's theory by treating the coupled vibrations of the solid in terms of 3N normal modes of vibration of all the system, each with its own frequency. The lattice vibrations are thus equivalent to 3N independent harmonic oscillators with these normal mode frequencies. For low frequency vibrations, defined as those for which the wavelength is much greater than the atomic spacing, $\lambda >> a$, the crystal may be treated as a homogeneous elastic medium. The normal modes are the frequencies of the standing waves that are possible in the medium.

Debye acquired a expression for the number of modes with frequency between ν and ν+dν in such a medium.

$$g(v)dv = \frac{4\pi V v^2}{V^3} dv = \alpha v^2 dv \tag{2.6}$$

Where V is the crystal volume and v is the propagation velocity of the wave. A_s outlined above, this expression applies only to low frequency vibrations in a crystal. Debye employed the approximation that it applied to all frequencies, and introduced a maximum frequency v_D (the Debye frequency) such that there were 3N modes in total. i.e. $\int_0^{v_D} g(v)dv = 3N$. The Debye frequency equals to $\lambda = 2\alpha$, when neighbouring atoms vibrate in antiphase with each other. With this approximation in place, Debye combined over all of the frequencies to find the internal energy of the crystal, afterwards calculated the heat capacity using $C_V = \left(\frac{\partial U}{\partial T}\right)_V$. The resulting expression is given below.

$$C_V = 3Nk\left(\frac{3}{{x_D}^3}\int_0^{x_D} \frac{x^4 e^x dx}{(e^x-1)^2}\right) \tag{2.7}$$

where $x = \frac{hv}{kT}$,and $x_D = \frac{hv_D}{kT} = \frac{\theta_D}{T}$. The Debye heat capacity depends only on the Debye temperature θ_D. The integral cannot be computed this expression analytically, but the bracketed function is categorized.

At high temperatures (T >>θ_D, x_D << 1), we may paraphrase the integrand as follows:

$$\frac{x^4 e^x}{(e^x-1)^2} = \frac{x^4}{(e^x-1)(1-e^x)} = \frac{x^4}{2(\cosh(x)-1)} = \frac{x^4}{2(x^2/2!+x^4/4!+\cdots)} \tag{2.8}$$

Retaining only the x^2 term in the denominator gives:

$$C_V = 3Nk\left(\frac{3}{{x_D}^3}\int_0^{x_D} x^2 dx\right) = 3Nk \tag{2.9}$$

To determine the low temperature limit (T << θ_D, x_D >> 1), we mark that the integrand inclines towards zero swiftly for large x. This allows us to change the place of the upper limit by ∞ and turn the integral into a standard integral, to give ;

$$C_V = 3Nk\left(\frac{T}{\theta_D}\right)^3 \left(3\int_0^{\infty} \frac{x^4 e^x}{(e^x-1)^2}\right) = \frac{12}{5}\pi^4 Nk\left(\frac{T}{\theta_D}\right)^3 \tag{2.10}$$

We observe that the Debye heat capacity decreases as T^3 at low temperatures, in agreement with experimental observation. This is a marked improvement on Einstein's theory.

2.3 Free Electron Model of Metals

Until this moment, we have only took into considerations of the contributions to the heat capacity from vibrations within the solid. In metals, the free conduction electrons also contribute to the heat capacity. In the free electron model of metals, the conduction electrons are treated as a perfect gas obeying Fermi-Dirac statistics. Interactions of the electrons with the positively charged atomic ions and with the other electrons are neglected. This is not such a bad approximation as it may appear at first: the ions provide a positively charged background that partly screens the electrons from each other; and the residual collisions are often relatively unimportant

- the energetically accessible final states are often already occupied, making any collisional excitation process forbidden by the Pauli exclusion principle.

The first step in deriving the heat capacity is to determine the density of states. We will first do this in momentum space, and then transform the result into an expression describing the density of states per unit energy.

The 3-dimensional Schrodinger equation for the translational motion of the electrons has the solutions ;

$$\phi_{n_1 n_2 n_3}(r) = A \sin\left(\frac{n_1 \pi x}{L}\right) \sin\left(\frac{n_2 \pi y}{L}\right) \sin\left(\frac{n_3 \pi z}{L}\right) \tag{2.11}$$

with $k = \left(\frac{\pi n_1}{L}, \frac{\pi n_2}{L}, \frac{\pi n_3}{L}\right)$ and $k^2 = \frac{\pi^2}{L^2}({n_1}^2 + {n_2}^2 + {n_3}^2)$

The allowed values of k thus form a cubic point lattice in k-space, with spacing π/L and volume per point $(\pi/L)^3$. Finding out the number of normal modes of the standing wave wavefunctions with k between k and k+dk is equivalent to finding the number of lattice points between two spherical shells of radii k and k+dk in the positive octant of k-space. The number of k-vectors of magnitude ≤ k is ;

$$n_k = \frac{volume\ of\ region}{volime\ per\ point} = \frac{(1/8)(4/3)\pi k^3}{(\pi/L)^3} = \frac{Vk^3}{6\pi^2} \qquad \text{where} \quad V=L^3 \tag{2.12}$$

The number f(k) within an interval dk is found by differentiating this expression, giving ;

$$f(k)dk = \frac{dn_k}{dk}dk = \frac{Vk^2 dk}{2\pi^2} \tag{2.13}$$

Since k = 2πp/h (and thus dk = (2π/h) dp), the density of states in momentum space is ;

$$f(p)dp = \frac{8\pi V p^2 dp}{h^3} \tag{2.14}$$

where an extra factor of two has been added to account for the two possible spin states of the electrons. This expression may be converted to an energy density of states by substituting ε = p^2/2m (and so dε = (p/m)dp), to give ;

$$f(\varepsilon)d\varepsilon = \frac{4\pi V}{h^3}(2m)^{3/2}\,\varepsilon^{1/2}\,d\varepsilon \tag{2.15}$$

To ascertain definitely the number of electrons with energies between ε and ε+dε, we need to multiply the above expression, which presents the density of states at energy ε, with the probability n(ε) of finding an electron in a given state with energy ε. Electrons are Fermions, and obey Fermi-Dirac statistics, so n(ε) is given by the Fermi-Dirac distribution (Note: the Fermi-Dirac distribution is an analogue of the Boltzmann distribution for systems in which spin must be taken into account);

$$n(\varepsilon) = \frac{1}{\exp[\beta(\varepsilon-\mu)]+1} \qquad \text{where } \mu \text{ is the chemical potential and } \beta=1/kT \tag{2.16}$$

The number of electrons with energy between ε and ε+dε is then

$$dN(\varepsilon) = n(\varepsilon)f(\varepsilon)d\varepsilon = \frac{1}{\exp[\beta(\varepsilon-\mu)]+1}\;\frac{4\pi V}{h^3}(2m)^{3/2}\,\varepsilon^{1/2}\,d\varepsilon \tag{2.17}$$

Integrating from zero to infinity gives the total number of electrons in the gas. The Fermi energy ε_F is the value of μ when T=0 i.e. ε_F = μ(0), and may also be writtenε_F = kT_F, where T_F is the Fermi temperature.

Now we will look at the energy level occupations n(e) and the overall energy distribution N(ε) as the temperature is increased from zero.

At T=0, the Fermi-Dirac distribution becomes ;

$$n(\varepsilon) = \frac{1}{\exp[\beta(\varepsilon-\varepsilon_F)]+1} \tag{2.18}$$

And since β=∞ at T=0, this is equal to 0 if ε > ε_F and 1 if ε < ε_F. The two distributions n(ε) and N(ε) are shown below (Figure 2.1).

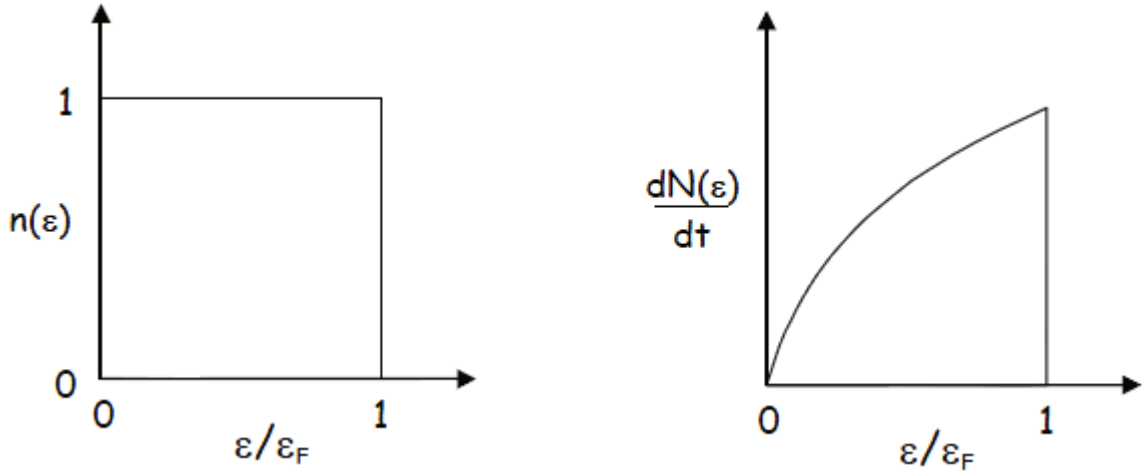

Figure 2.1 The Two Distributions n(ε) and N(ε)

At higher temperatures, the two distributions alter slightly from their behaviour at T=0, due to electrons lying below the Fermi level being excited to states lying above the Fermi level. This is shown below (Figure 2.2).

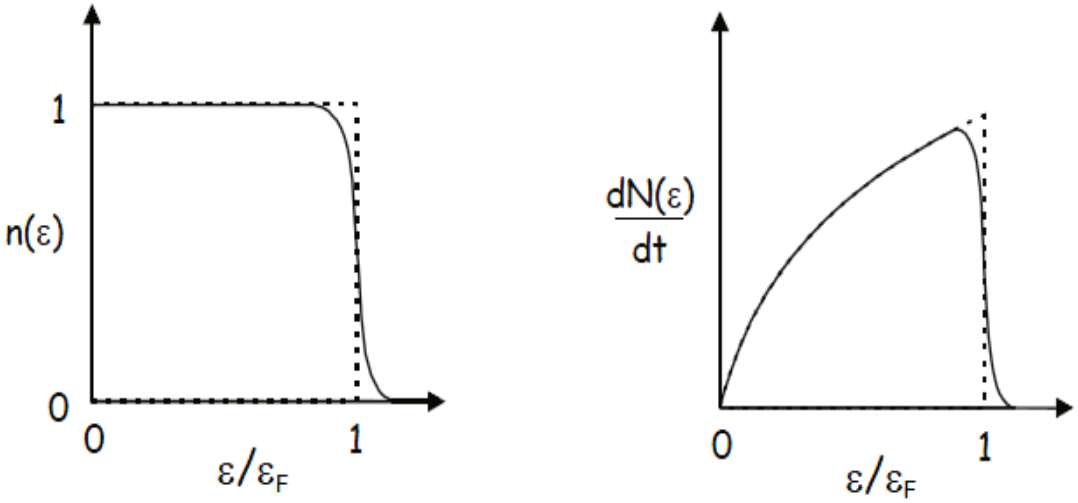

Figure 2.2 The Two Distributions Alter Slightly from Their Behaviour at T=0

At the moment, we will consider the results of these distributions for the heat capacity. Classical mechanics would predict a contribution ½ kT per electron to the heat capacity, in addition to the heat capacity arising from the lattice vibrations. This is a much larger contribution than is observed experimentally. The answer lies in the Fermionic nature of the electrons. In the classical model, a change in temperature ΔT would lead to an energy increase of around kΔT per electron. Nonetheless, we have seen that apart from electrons with energies very close to the Fermi energy εF, the states to which the electrons would be promoted by an energy increase of this magnitude are already occupied. Hence, only a very small fraction of electrons, those lying within ~kΔT of the Fermi level, are able to absorb the energy and contribute to the heat capacity.

The heat capacity per electron turns out to be ;

$$C_V = \frac{\pi^2}{2} k \frac{T}{T_F} \tag{2.19}$$

At room temperature this is a very small contribution to the overall heat capacity (on the order of a few percent). Nevertheless, at very low temperatures the electronic heat capacity dominates, since it is linear in temperature while the lattice heat capacity is proportional to T^3.

CHAPTER THREE

MATERIALS AND METHODS

3.1 Materials and Methods

3.1.1 HDPE/Graphite

The matrix material (fabricated in Petkim Petrokimya Holding A.Ş.) is a high-density polyethylene with a density of 0.966 0.970 g/cm^3 at 23ºC and a melt flow rate is 4.4-6.5g/10 min (at 190ºC, 2.16 kg). It is in powder form and its commercial name is Petilen I 668 (UV). As a graphite powder which is produced in NanoAmor with particle size 30 nm , the metallic filler is with a density of 2.25 g/cm^3 at 20ºC. HDPE is produced by catalytic polymerization of ethylene in either slurry (suspension), solution or gas phase reactors. In the modulation of the quality of the product, the selection of catalyst and/or the use of biomodal processes are employed. HDPE is a thermosetting white solid. In addition, this thermosetting white solid has molecular chains which are quite straight and nearly ordered. (Figure 3.1) It can resist to the most chemicals, insoluble in organic solvents with its high impact and tensile strength. HDPE is the third largest commodity thermoplastic. A major outlet for HDPE is in blow-moulding applications such as bottles, packaging containers, drums, fuel tanks for automobiles, toys and house wares. Crates, pallets, packaging containers and caps, paint cans, house wares and toys are included in HDPE which is made from injection-moulded. In many countries there is a global demand and this demand has been getting higher and stronger in a reasonable manner. Future global growth is assumed to be around 5%/year. (Polyethylene - high density (HDPE)).

There is two natural crystalline allotropic form of carbon: graphite and diamond. Graphite is generally greyish-black, blurred and has a bright black lucent (Figure 3.1) Graphite has matchless characteristics because its property is both metal and non-metal. It has a high thermal and electrical conductivity. Another characteristics of graphite is its being flexible but not elastic. Moreover, it is highly refractory and chemically inert. It has a low adsorption of X-rays and neutrons. This enables it

especially utile material in nuclear field. (Graphite's properties) There are two essential categorizations of graphite: natural and synthetic.

Table 3.1 Properties of polymer matrix, HDPE (Petkim)

Property	**Unit**	**Valume**	**Test Method**
Melt Flow Rate (*2160g, 190°C)*	g/10 min	4.4-6.5	ASTM D1238
Density, 23°C	g/cm^3	0.963 - 0.967	ASTM D1505
Tensile Strength			
- At Yield	Mpa	30	ASTM D638
- At Break	Mpa	17	ASTM D638
- Elongation At Break	%	1250	ASTM D638
Stiffness	Mpa	1100	TS EN ISO 178
Izod Impact Strength	J/m	50	ASTM D256
ESCR, (F50)	Hour	4	ASTM D1693

Natural graphite as a mineral contains graphitic carbon. It becomes varied in a considerable extent in crystallinity. It is separated into three subdivisions: amorphous, flake and high crystalline. Synthetic graphite can be produced from coke and pitch. It is inclined to be of higher purity, however, it does not have characteristics of crystalline as natural graphite.

In metallurgy, pencil production, refractoriness, coatings, lubricants, paint production, making batteries, grinding wheels, powder metallurgy, secondary steel making and fabrication of graphite foil, natural graphite has been applied. Synthetic

graphites are employed in aerospace applications, batteries, carbon brushes, graphite electrodes for electric arc furnaces for metallurgical processing and moderator rods in nuclear power plant. (Graphite's properties).

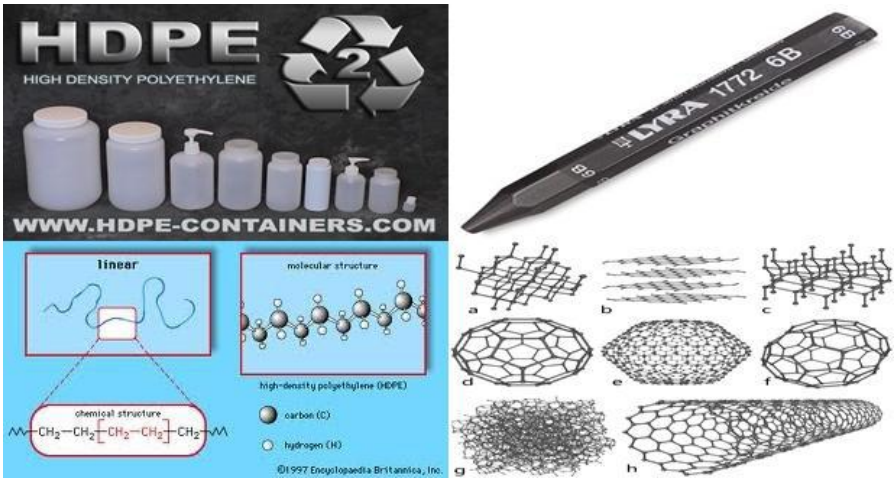

Figure 3.1 Graphite-HDPE and their chemical formulas. (image above is from Nanoage)

In different weight contents (4, 6, 8, 10, 12, 15, 17, 20, 22 %) of graphite/HDPE nanocomposites were produced. First of all, for 6 hours graphite was dried. By means of mold compression process, samples arranged. HDPE and graphite powders are mixed in a Brabender Plasticorder W30 internal mixer at 180°C for a total mixing time of 10 min, the mixing chamber capacity is 30 ml. (Figure 3.2) The rotors were turned at 35 rpm for 15 minutes at 180°C. Afterwards, the mixed powder was melted under pressure in a mold and solidified by aircooling. The process conditions were molding temperature of 180ºC and pressure of 40kPa for 1 minute. The resulting samples for thermal conductivity measurements are annular in shape of 15 mm diameter and 10 mm thickness due to the measuring probe.

Figure 3.2 General view Brabender Plasticorder W30/The mixing chamber and the rotors after the mixing process of the composite (Tavman et al., 2008).

3.1.2 Measurement System of Differential Scanning Calorimetry (DSC)

Thermal analysis is an analysis method in which a physical property of the sample is studied as a function of temperature or in a reaction absorbed or released heat is followed. The main methods, which are similar to DSC method, differential thermal analysis (DTA), differential scanning calorimetry (DSC), thermometric titration and direct injection entalpimeter. Of course, if we talk about mentioned differential scanning calorimetry method:

Since thermal analysis are mostly held under constant pressure, valid Gibbs-Helmholtz thermodynamic equation:

$$dG = dH - TdS \tag{3.1}$$

Here, G is the free energy of the system, h is enthalpy of system, S is entropy of the system and T is Calvin temperature. Methods like TG, DTA and DSC in which temperature is independent variable, term is important. If equation of Gibbs-Helmholtz according to temperature is taken:

$$d(dG)/dT = dS \tag{3.2}$$

will be found. Through this equation, it is shown that how to overcome from a state, where reaction does exist (dG>0), to a state where reaction exists (dG <0). Positive will be negative by the increase of temperature. If it is negative, reaction which is by itself will be obtained with the decrease of temperature. Once the reaction starts, three of these methods can be used to observe.

In DSC method, while the same temperature program is applied to material and reference substance, in case of any change in material, same temperature is provided by giving temperature with the help of an electric circuit. DSC curves are drawn graphics of curves added heat against the temperature. The area reaction seen here, which is under the peak; heat absorbed or released by the peak heights is directly proportional to the reaction rate. If dH is negative (exothermic), temperature is added to reference heater and a negative signal is obtained. The integral of these peaks depends on the amount of temperature the sample gives or takes. DSC is very sensitive not only to incident of change of enthalpy but also to difference between the heat capacities of reference and sample.

By DSC, a lot of material's characteristics like enthalpy, crystallization temperature, the glass transition temperature, thermal stability, purity, and curie temperature can be examined.

3.1.2.1 Principles of Specific Heat Capacity Measurement

Figure 3.3 shows an example of acquiring specific heat capacity using DSC. The measurements conductions for sample , the reference (a sample with a known specific heat capacity) and the empty pan were the same. The specific heat capacity of the sample was calculated by equation 1 from the DSC data obtained (a,b,and c in figure)

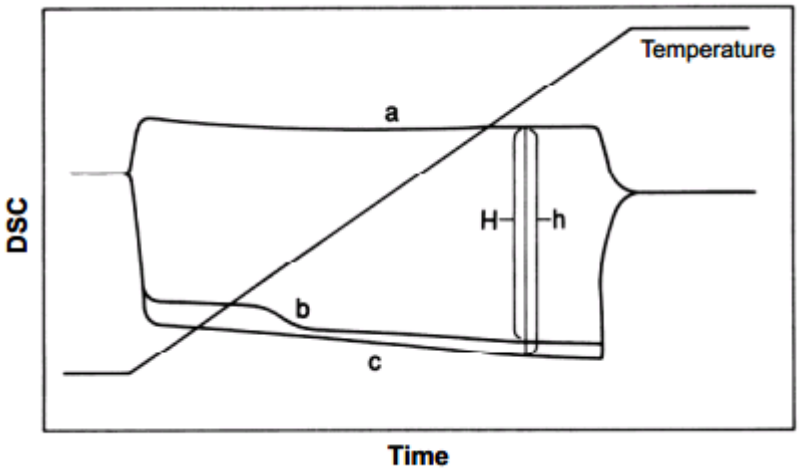

Figure 3.3 DSC Measurement of Specific Heat Capacity (a: empty pan , b: sample, c: reference

$$C_{p_s} = \frac{H}{h}\ \frac{m_r}{m_s}\ C_{p_r} \tag{3.3}$$

Where C_{p_s} C_p of sample , C_{p_r} C_p of reference , m_s weight of sample , m_r weight of refence, H difference of sample and empty pan, h difference of reference and empty pan.

3.1.3 Experimental Set-up

In our experimental work, Cp measurement has been done by using the device of DSC. In order to measure the specific heat capacity by DSC, graphite filled with polymer nanocomposites ,which is produced in Petkim, (figure 3.4) have been pretreated. This process can be narrated in this way:

Figure 3.4 Graphite Filled with Polymer Nanocomposites

We have placed the specimen (produced in Petkim) among the metal plates with flat surfaces homogenously. The specimen, placed among the metal plates by the aid of hot-press (figure 3.5 and 3.6) method, is pressed heating to the degree of 400-415 K gradually till the specimen reaches to 1mm thickness step by step. The resulting specimen, which is 1 mm in thickness, has been cut in an appropriate dimension and mass to be able to use in DSC. Before and after the measurement of the specimen in DSC, their masses are measured via precision balance. The whole process is applied for all the specimens.

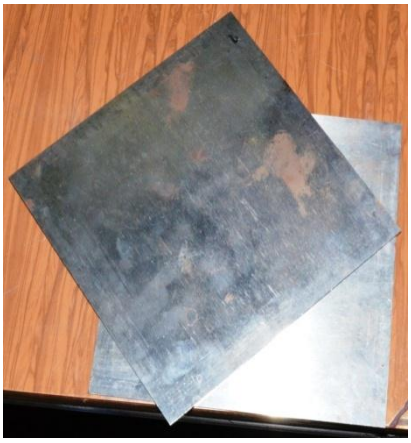

Figure 3.5 Metal Plates

Figure 3.6 Hot-Press

3.1.3.1 Heat Capacity Measurements

The heat capacity measurement of the samples was carried out at a heating rate of 10ºC/min between -10ºC and 200ºC temperature range. For these measurements Perkin Elmer Diamond DSC (Differential Scanning Calorimeter) was used. The heat flow curves of the empty container, standard material (sapphire) and samples were obtained at the following temperature levels for determining the heat capacity (Cp):

1) 2 min. isothermal at 0ºC,

2) Increasing temperatures by a heating rate of 10ºC/min from -10ºC to 200ºC,

3) 2 min. isothermal at 200ºC.

Taking into account these three levels, at first the measurements were carried out by placing the two aluminum empty container and cover into sample and reference parts of the DSC furnace to determine the heat flow curve (baseline) of empty container. Secondly the standard material curve was obtained by placing the standard material (sapphire) in empty container taken place sample part. Finally the sample heat flow curve was obtained by placing sample in sample part. The temperature dependence of heat capacity was determined from these curves by Pyris 8.0 standard analysis program (Tavman et al., 2011).

CHAPTER FOUR

RESULTS AND DISCUSSION

Heat capacity of HDPE/graphite composites in a very close linear decrease with the increasing volume content of graphite in the composite. Experimental results and the result of theoric equation (Eq 4.1) of specific heat are explained in the figure 4.1 and table 4.1. The datum gained by means of experiment are very close to the results of teoric equation.

Similarly, Tavman et al., 2011 came to the conclusion that heat capacity decrease with increasing weight concent in the study named *Measurement of heat capacity and thermal conductivity of HDPE/expanded graphite nanocomposites by differential scanning calorimetry.*

Table 4.1 Specific heat capacity results (J/kg K)

Particle weight concent	Particle vol. concent.	Cp model Eq (4.1)	**Cp** HDPE EG
0,00	0,000	1847,0	1847
0,04	0,018	1801,8	1845
0,06	0,027	1778,5	1801
0,08	0,036	1756,7	1725
0,10	0,046	1733,0	1711
0,12	0,056	1710,0	1674
0,15	0,071	1676,4	1606
0,17	0,081	1654,7	1634
0,20	0,097	1621,0	1530
0,22	0,108	1598,6	1554

As it is observed in the table 4.2 and figure 4.2, the density of composites increases with increasing graphite fraction (vol).

$$C_p = \phi_{wt}\, C_{p_f} + (1 - \phi_{wt})\, C_{p_m} \tag{4.1}$$

where, C_p: theoretical specific heat, ϕ_{wt}: weight portion of the filler, C_{p_f} : filler specific heat, C_{p_m} : matrix specific heat.

$$\phi_{vol} = \left[1 + \left({\phi_{wt}}^{-1} - 1\right)\left({\rho_f}/{\rho_m}\right)\right]^{-1} \tag{4.2}$$

$$\rho = \left(\rho_f - \rho_m\right)\phi_{vol} + \rho_m \tag{4.3}$$

where, ϕ_{vol}: volume content, ϕ_{wt}: weight portion, ρ: composite density, ρ_f: filler density, ρ_m: matrix density.

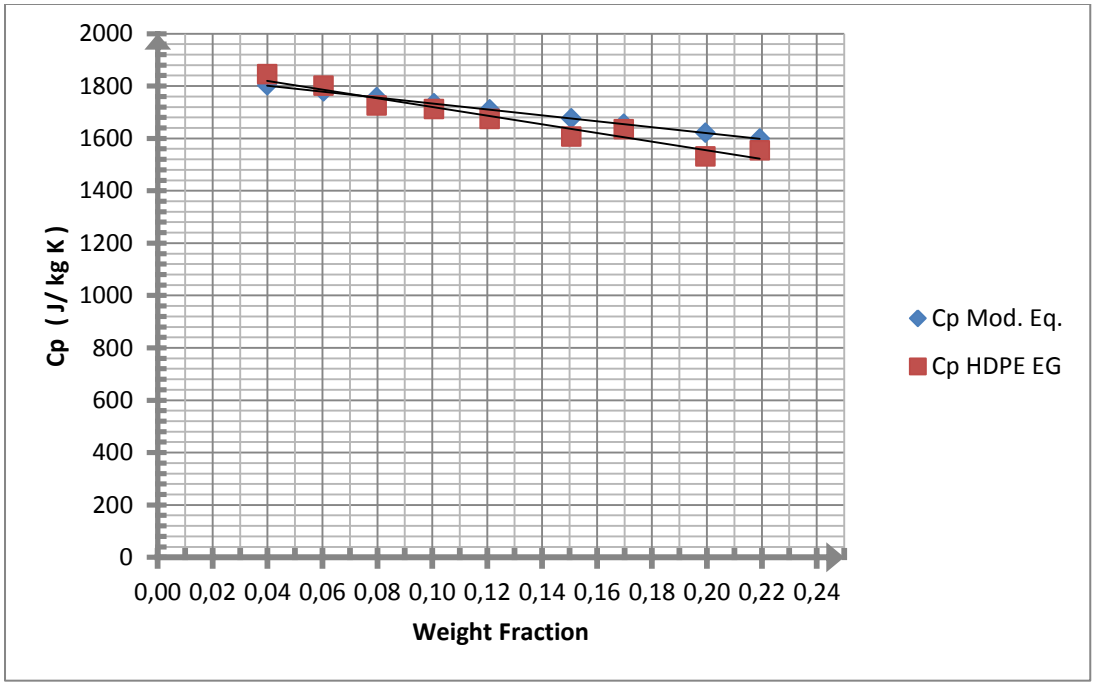

Figure 4.1 Specific heat capacity versus filler weight fraction for HDPE-EG30 and Eq. 4.1 samples.

Table 4.2 Density of composite (kg/m^3).

ϕ_{wt}	ϕ_{vol}	$\rho_{composite}$
0,04	0,018	992,528
0,06	0,027	1004,56
0,08	0,036	1016,08
0,10	0,046	1028,88
0,12	0,056	1041,68
0,15	0,071	1060,88
0,17	0,081	1073,68
0,20	0,097	1094,16
0,22	0,108	1108,24

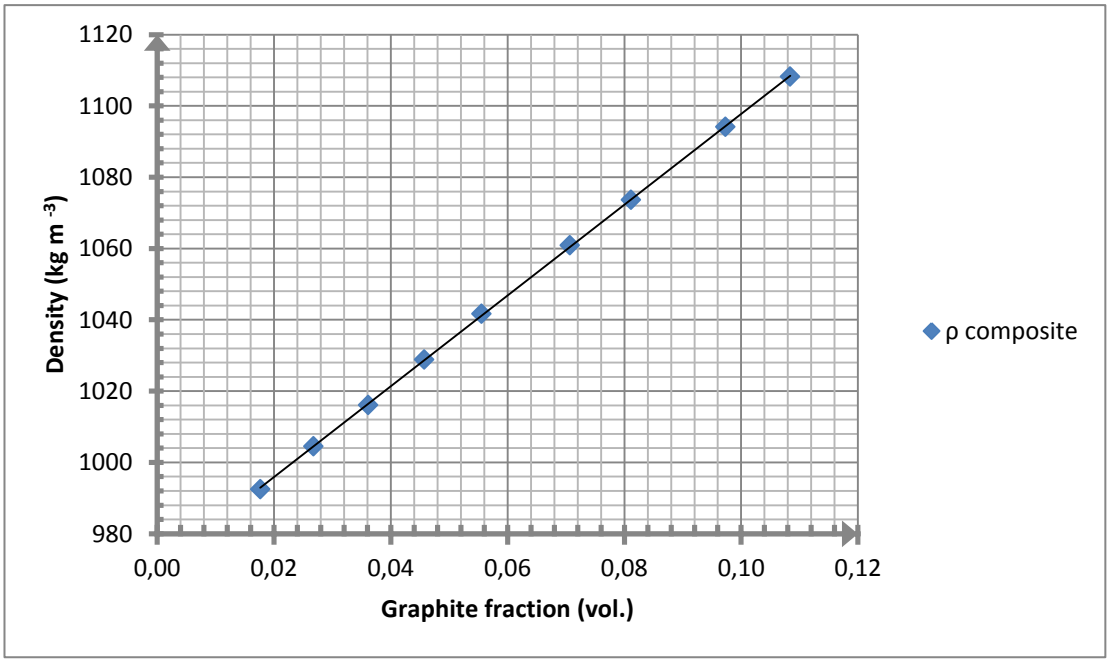

Figure 4.2 Density of composite Depending on the Amount of Graphite Increased.

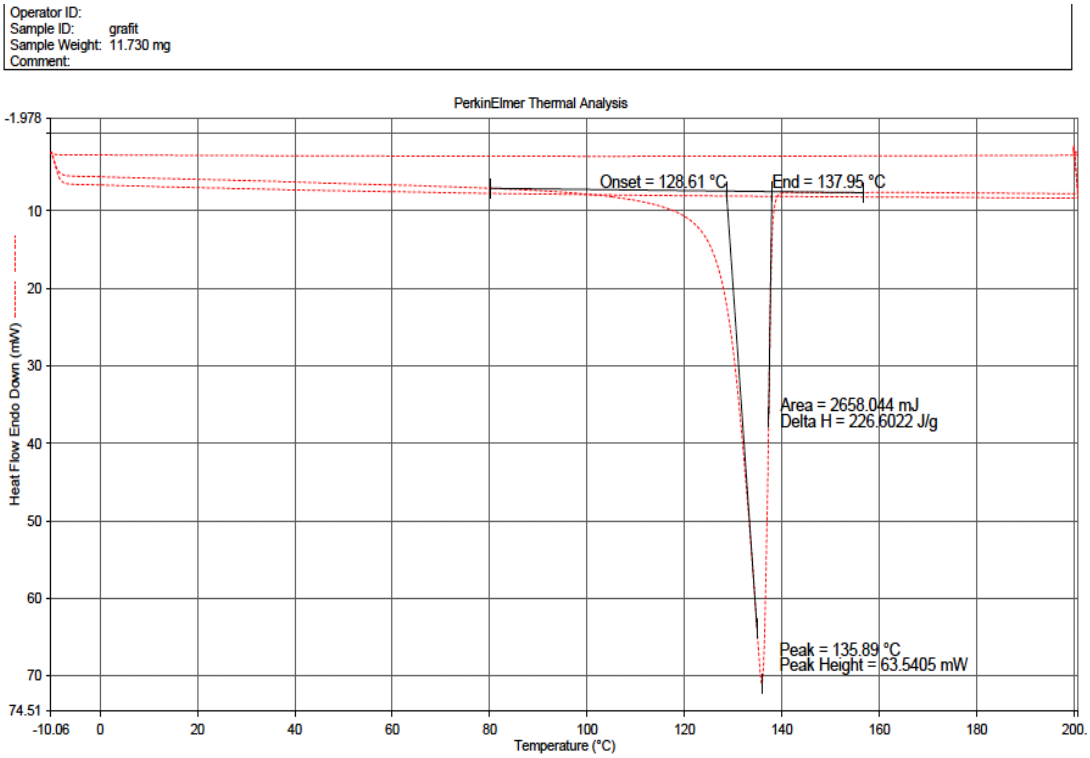

Figure 4.3 DSC analysis result of % 4 graphite filled polymer nanocomposite.

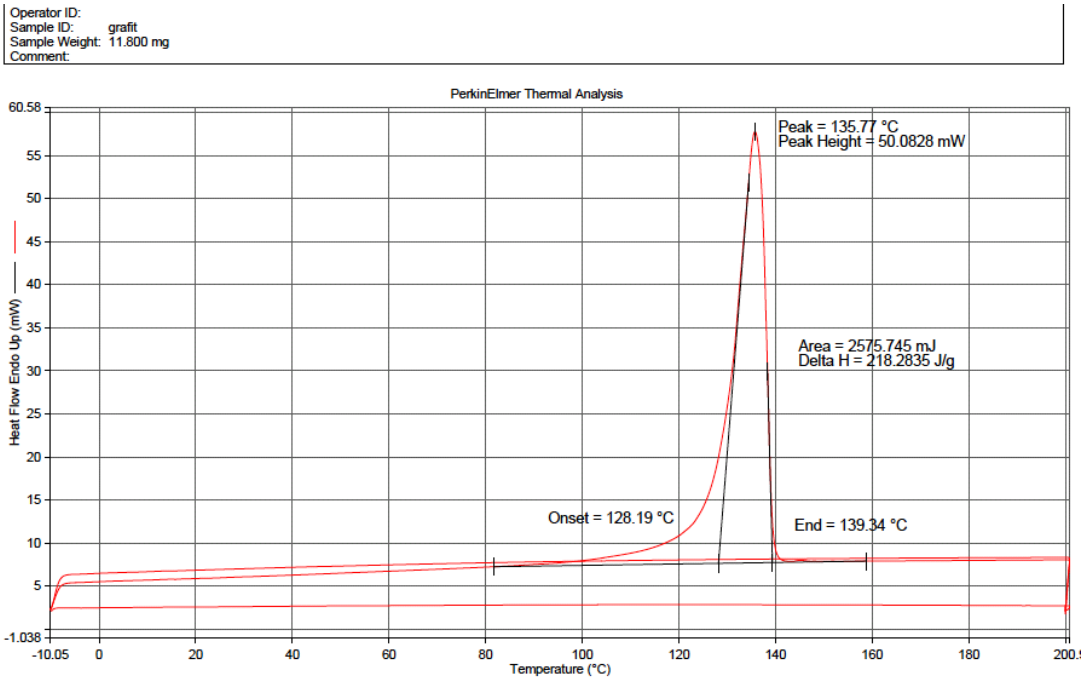

Figure 4.4 DSC analysis result of % 6 graphite filled polymer nanocomposite.

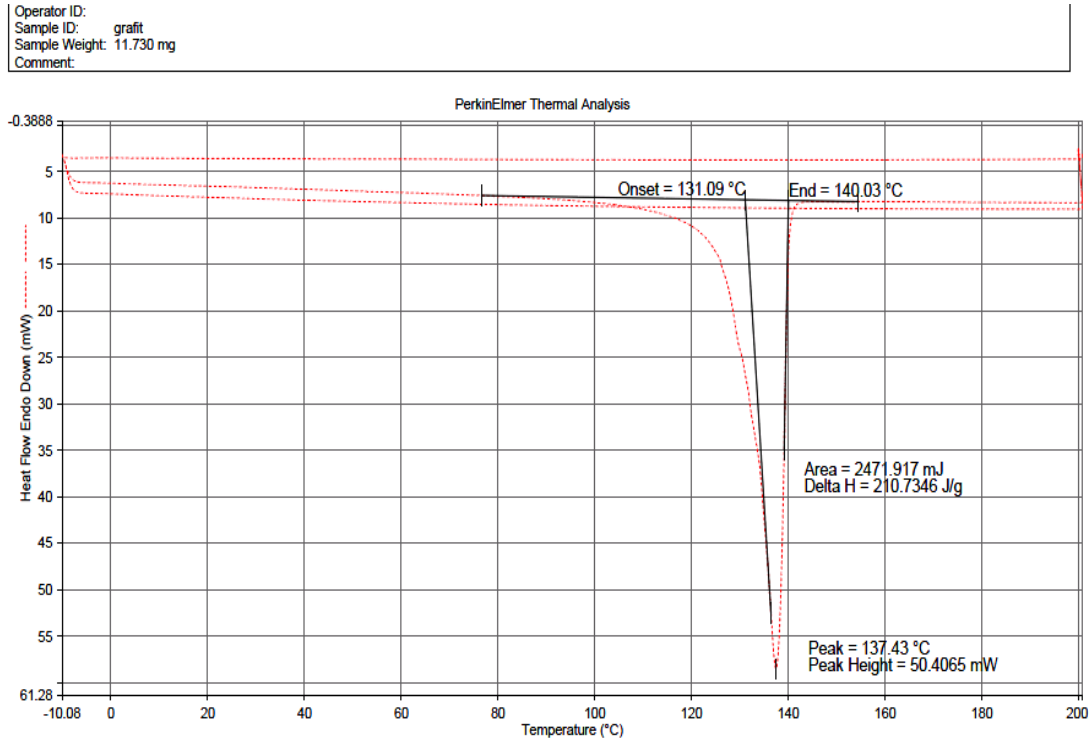

Figure 4.5 DSC analysis result of % 8 graphite filled polymer nanocomposite.

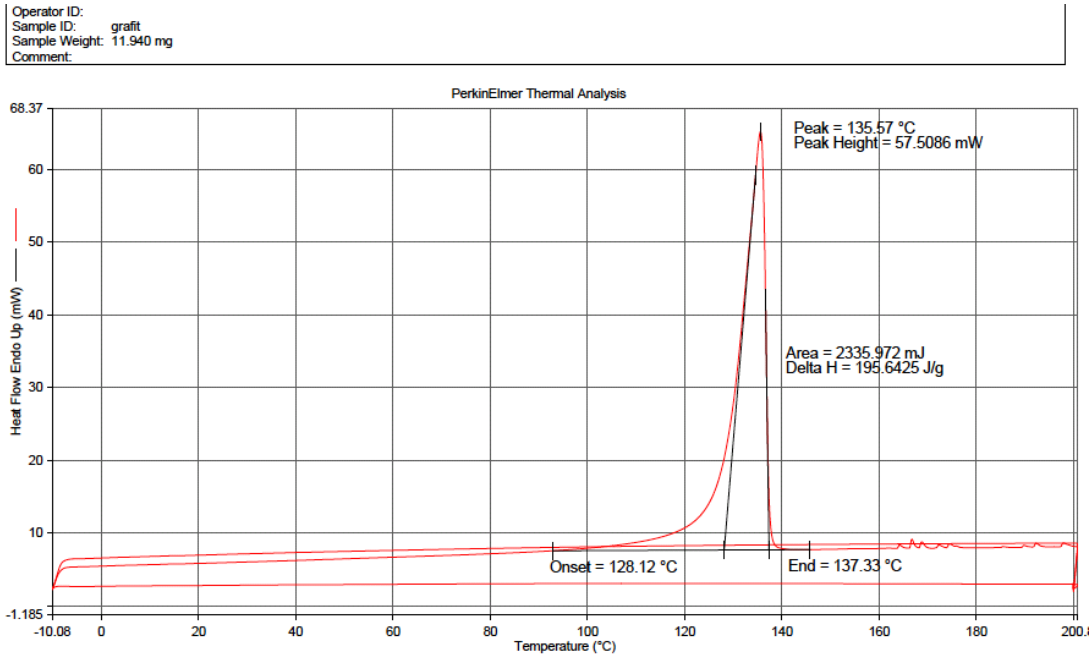

Figure 4.6 DSC analysis result of % 10 graphite filled polymer nanocomposite.

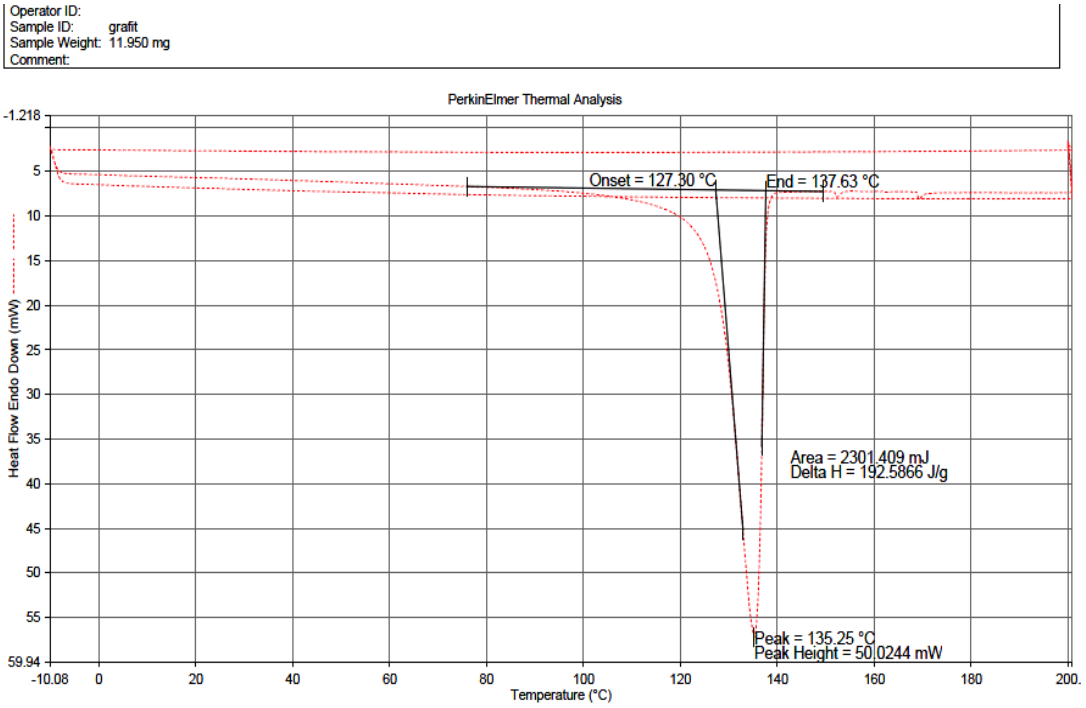

Figure 4.7 DSC analysis result of % 12 graphite filled polymer nanocomposite.

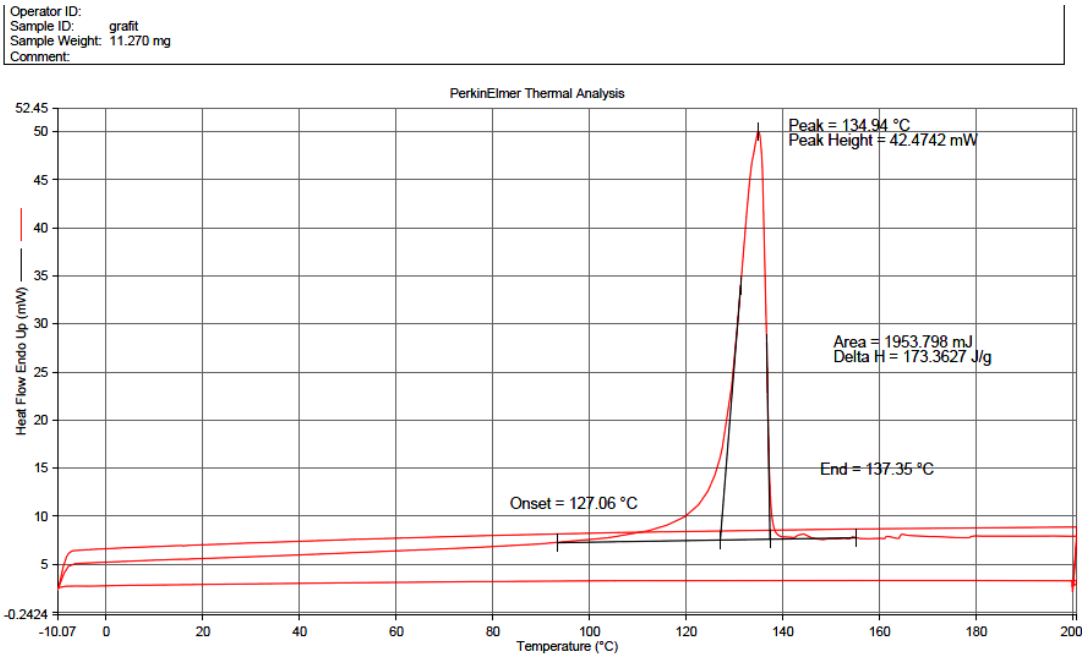

Figure 4.8 DSC analysis result of % 15 graphite filled polymer nanocomposite.

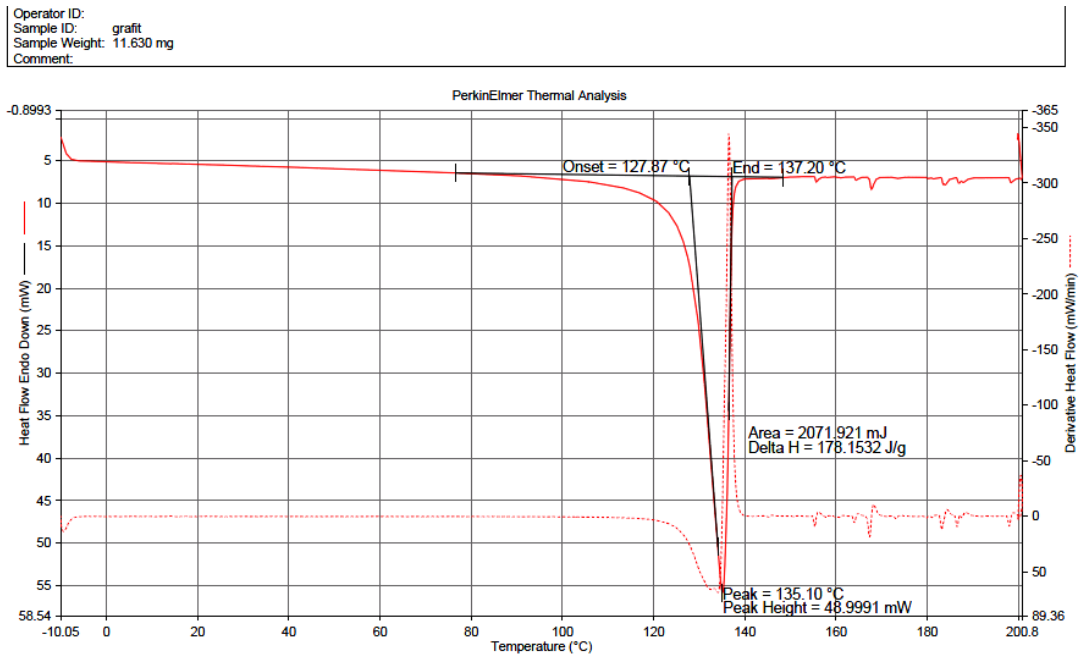

Figure 4.9 DSC analysis result of % 17 graphite filled polymer nanocomposite.

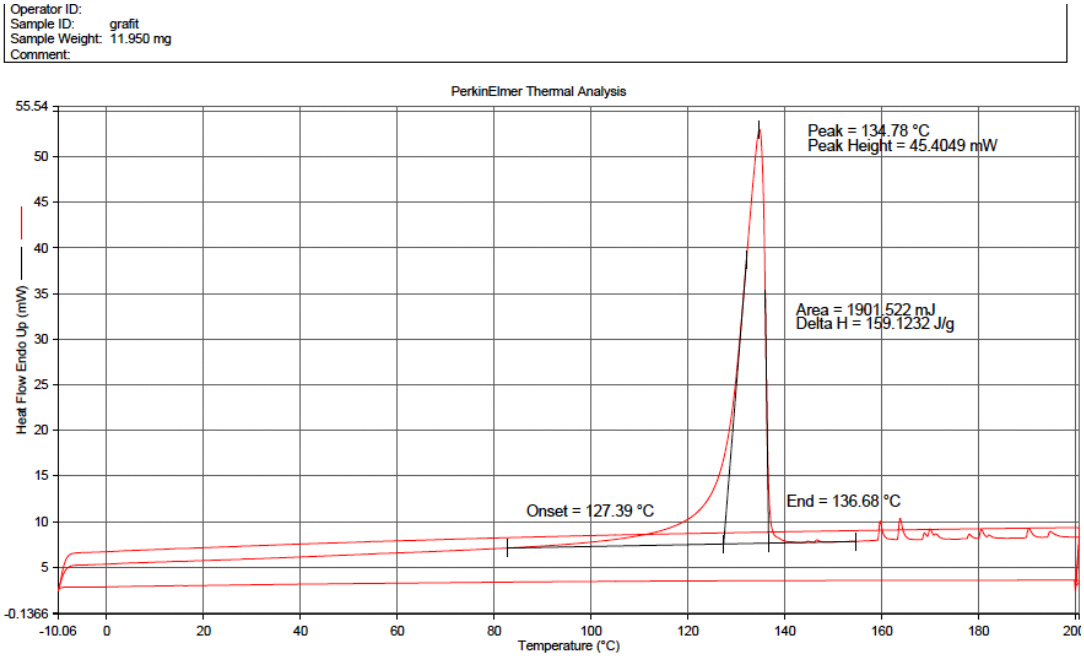

Figure 4.10 DSC analysis result of % 20 graphite filled polymer nanocomposite.

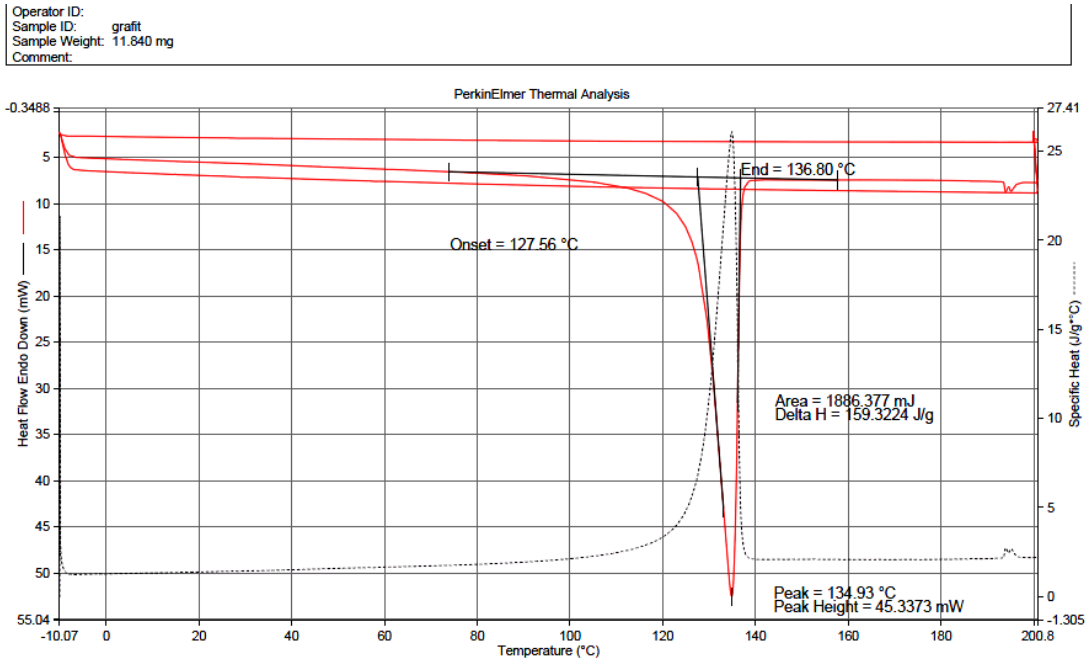

Figure 4.11 DSC analysis result of % 22 graphite filled polymer nanocomposite.

Table 4.3 DSC analysis results of graphite filled polymer nanocomposites.

Volume Fractions (%)	**T_m (°C)**	**Δh_m (J/g)**
4	135.89	226.602
6	135.77	218.283
8	137.43	210.734
10	135.57	195.642
12	135.25	192.586
15	134.94	173.362
17	135.10	178.153
20	134.78	159.123
22	134.93	159.322

CHAPTER FIVE

CONCLUSIONS AND FUTURE REMARK

Graphite powder (30 nm) was mixed with HDPE in the Brabender Plasticorder mixer. Nanocomposites containing (4,6,8,10,12,15,17,20,22 %) weight fractions of graphite were fabricated. To learn heat capacity, these samples were measured by DSC (Differential Scanning Calorimetry) and with the increasing volume content of graphite it was observed that heat capacities were decrease nonlinearly, it was similar as in the literature.

Even the addition of small proportions of filler materials, they decrease the heat capaciyt of composites.

In the future, studies must focus on making theoretical models that fit most new composites, have general validity for all composites.

REFERANCES

Abdel-Aal, N., El-Tantawy, F., Al-Hajry, A. & Bououdina, M. (2008). Epoxy resin/plasticized carbon black composites. Part I. Electrical and thermal properties and their applications, *Polymer Composites, vol.29*, pp. 511–517.

Boudenne, A., Ibos, L., Fois, M., Majeste, J.C. & Géhin, E. (2005). Electrical and thermal behavior of polypropylene filled with copper particles. *Composites: part A, vol.36*, pp. 1545–1554.

Causin, V., Marega, C., Marigo, A., Ferrara, G. & Ferraro, A. (2006). Morphological and structural characterization of polypropylene/conductive graphite nanocomposites. *European Polymer Journal, vol.42*, pp. 3153–3161.

Chan, C.M., Wu, J., Lı, J.X., Cheung, Y.K., (2002). Polypropylene/calcium carbonate nanocomposites. *Polymer. Vol.43,* pp. 2981-2992.

Chen, N., Wan, C., Zhang, Y., (2004). Effect of nano-CaCO3 on mechanical properties of PVC and PVC/Blendex blend. *Polymer Testing, Vol. 23*, pp. 169-174.

Chen, Y. & Ting, J., (2002). Ultra high thermal conductivity polymer composites. *Carbon, vol.40*, pp. 359–362.

Cho, J.W., Joshi, M.S., Sun, C.T., (2006). Effect of inclusion size on mechanical properties of polymeric composites with micro and nano particles. *Composites Science and Technology, Vol. 66*, pp. 1941-1952.

Cho, J.W., Paul, D.R., (2001). Nylon-6 nanocomposites by melt compounding. *Polymer, Vol. 42*, pp. 1083-1094.

Du, F., Scogna, R.C., Zhou, W., Brand, S., Fischer, J.E., Winey, K.I, (2004). Nanotube networks in polymer nanocomposites: rheology and electrical. *Macromolecules, Vol. 37,* pp. 9048-9055.

Durmuş, A., (2006). *Poliolefin Nanokompozitlerin Hazırlanması*, İstanbul University. Graduate School of Natural and Applied. Thesis (PhD).

Ebadi-Dehaghani, H. and Nazempour, M. (2012). *Thermal Conductivity of Nanoparticles Filled Polymers*, Smart Nanoparticles Technology, Dr. Abbass Hashim (Ed.), ISBN: 978-953-51-0500-8. Retrieverd 20 july 2012 from: http://www.intechopen.com/books/smart-nanoparticles-technology/thermal-conductivity ofnanoparticles- filled-polymers.

Fouad, H., Elleithy, R., Al-Zahrani, S.M., Al-haj, Ali M., (2011). Characterization and processing of High Density Polyethylene/carbon nano-composites. *Materials and Design, vol 32*, pp. 1974–1980.

Ganguli, S., Roy, A.K. & Anderson, D.P., (2008). Improved thermal conductivity for chemically functionalized exfoliated graphite/epoxy composites. *Carbon, vol.46*, pp. 806–817.

Gao, F., (2004). Clay/polymer composites: the story. *Materials Today*, November, pp. 50-55.

Giannelis, E.P., (1996). Polymer Layered Silicate Nanaocomposites. *Advanced Materials, Vol. 8*, pp. 29-35.

Gu, J., Zhang, Q., Dang, J., Zhang, J. & Yang, Z., (2009). Thermal conductivity and mechanical properties of aluminum nitride filled linear low-density polyethylene composites. *Polymer Engineering Science, vol.49*, pp. 1030–1034.

Hasan, M., Zhou, Y., Mahfuz, H., Jeelanı, S., (2006). Effects of SiO_2 nanoparticles on the thermal and tensile behavior of nylon-6. *Materials Science and Engineering A,Vol.429,* pp. 181-188.

He, H., Fu, R., Han, Y., Shen, Y. & Song, X., (2007). Thermal conductivity of ceramic particle filled polymer composites and theoretical predictions. *Journal of Material Science, vol.42,* pp.6749–6754. DOI 10.1007/s10853-006-1480-y.

Holıster, P., Weener, J.W., Vas, C.R., Harper, T., (2003). *Nanoparticles*, Cientifica Ltd., Technology White Papers (3), Retrieved 29 july from: http://images.iop.org/dl/nano/wp/nanoparticles_WP.pdf

Hussaın, F., (2006). Review article: polymer-matrix nanocomposites, processing, manufacturing and application: an overview. *Journal of Composite Materials, Vol.40,* pp. 1511-1576.

Ishida, H. & Rimdusit, S. (1998). Very high thermal conductivity obtained by boron nitridefilled polybenzoxazine. *Thermochimica Acta, vol.320,* pp. 177–186.

King, J.A., Morrison, F.A., Keith, J.M., Miller, M.G., Smith, R.C., Cruz, M., Neuhalfen, A.M. & Barton, R.L., (2006). Electrical conductivity and rheology of carbon-filled liquid crystal polymer composites. *Journal of Applied Polymer Science, vol.101*, pp. 2680– 2688.

Knauert, S.T., Douglas, J.F., Starr, F.W., (2007). The effect of nanoparticle shape on polymer-nanocomposite rheology and tensile strength. *Journal of Polymer Science: Part B: Polymer Physics, Vol. 45*, pp. 1882-1897.

Knite, M., Teteris, V., Kiploka, A., Kaupuzs, J., (2004). Polyisoprene-carbon black nanocomposites as tensile strain and pressure sensor materials. *Sensors and Actuators A: Physical, Vol. 110,* pp. 142-149.

Krupa, I., Novák, I., Chodák, I., (2004). Electrically and thermally conductive polyethylene/graphite composites and their mechanical properties. *Synthetic Metals, vol. 145*, pp. 245–252.

Krupa, I., Chodák, I., (2001). Physical properties of thermoplastic/graphite composites. *Europen Polymer Journal, vol. 37*, pp. 2159-2168.

Kumlutas, D., Tavman, I. H. & Coban, M.T., (2003). Thermal conductivity of particle filled polyethylene composite materials. *Composites Science and Technology, vol.63*, pp.113– 117.

Kuriger, R.J., Alam, M.K., Anderson, D.P. & Jacobsen, R.L., (2002). Processing and characterization of aligned vapor grown carbon fiber reinforced polypropylene. *Composites: PartA, vol.33*, pp. 53–62.

Leodidou, T.K., Margraf, P., Caseri, W., Suter, U.W., Walther, P., (1996). Polymer sheets with at thin nanocomposite layer acting as a UV filter. *Polymers For Advenced Technologies, Vol. 8*, pp. 505-512.

Liang, Z.M., Wan, C.Y., Zhang, Y., Weı, P., Yın, J., (2004). PVC/montmorillonite nanocomposites based on a thermally stable, rigid-rod aromatic amine modifier. *Journal of Applied Polymer Science, Vol.92,* pp. 567-575.

Lim, Y.T., Partk, O.O., (2001). Phase morphology and rheological behavior of polymer layered silicate nanocomposites. *Rheologica Acta, Vol. 40*, pp. 220-229.

Liu, Z., Guo, Q., Shi, J., Zhai, G. & Liu, L., (2008). Graphite blocks with high thermal conductivity derived from natural graphite flake. *Carbon, vol.46,* pp. 414–421.

Magaraphan, R., Lılayuthalert, R., Sırıvat, A., Schwank, J.W., (2001). Preparation, structure, properties and thermal behavior of rigid-rod polyimide/montmorillonite nanocomposites. *Composite Science and Technology, Vol. 61*, pp. 1253-1264.

Mamunya, Y.P., Davydenko, V.V., Pissis, P. & Lebedev, E.V., (2002). Electrical and thermal conductivity of polymers filled with metal powders. *European Polymer Journal, vol.38*, pp. 1887–1897.

Mohammed, H.A. & Uttandaraman, S., (2009). A review of vapor grown carbon nanofiber/polymer conductive composites. *Carbon, vol.47*, pp. 2–22.

Mu, Q., Feng, S. & Diao, G., (2007). Thermal conductivity of silicone rubber filled with ZnO. *Polymer Composites, vol.28*, pp. 125–130.

Ohashi, M., Kawakami, S. & Yokogawa, Y., (2005). Spherical aluminum nitride fillers for heatconducting plastic packages. *Journal of American Ceramic Society, vol.88*, pp. 2615– 2618.

Ozmusul, M. S., (2006). *Nanoscale structure and mechanical behavior of plymer nanocomposites*, Rensselaer Polytechnic Institute. Thesis (PhD).

Park, S.H., Hong, C.M., Kim, S. & Lee, Y.J., (2008). Effect of fillers shape factor on the performance of thermally conductive polymer composites, *ANTEC Plastics - Annual Technical Conference Proceedings 2008*, pp. 39–43.

Peng, Z., Kong, L.X., (2007). A thermal degradation mechanism of polyvinyl alcohol/silika nanocomposites. *Polymer Degradation and Stability, Vol. 92*, pp. 1061- 1071.

Pierson, H.O. (1993). *Handbook of carbon, graphite, diamond and fullerenes: properties*. Processing and applications, Noyes Publications, New Jersey.

Pryamıtsyn, V., Ganesan, V., (2006). Mechanisms of steady-shear rheology in polymer-nanoparticle composites. *Journal of Rheology*. Vol. 50, pp. 655-683.

Qıan, J., He, P., Nıe, K., (2004). Nonisothermal crystallization of PP/nano-SiO_2 composites. *Journal of Applied Polymer Science, Vol. 91*, pp. 1013-1019.

Ray, S.S., Okamoto, M., (2003). Polymer/layered silicate nanocomposites: a review from preparation to processing. *Progress in Polymer Science, Vol. 28*, pp. 1539-1641.

Ray, S.S., Bousmina, M., (2005). Poly(butylene sucinate-co-adipate)/ montmorillonite nanocomposites: effects of organic modifier miscibility on structure, properties and viscoelasticity. *Polymer, Vol. 46*, pp. 12430-12435.

Roy, M., Nelson, J.K., Maccrone, R.K., Schadler, L.S., Reed, C.W., Keefe, R., (2005). Polymer nanocomposite dielectrics- the role of the interface. *IEEE Transaction on Dielectric and Electrical Insulation, Vol. 12*, pp. 629-643.

Sarikanat, M., Sever, K., Erbay, E., Güner, F., Tavman, I.H., Turgut, A., Seki, Y., Özdemir, I., (2011). Preparation and mechanical properties of graphite filled HDPE nanocomposites. *Archives of Materials Science and Engineering, vol 50*, pp. 120-124.

Stankovich, S., Dikin, D.A., Dommett, G.H.B., Kohlhaas, K.M., Zimney, E.J., Stach, E.A., Piner, R.D., Nguyen, S.T. & Ruoff, R.S., (2006). Graphene-based composite materials. *Nature, vol.442*, pp. 282–286.

Sun, S., Li, C., Zhang, L., Du, H., Gray, J.S.B., (2006). Interfacial structures and mechanical properties of PVC composites reinforced by $CaCO_3$ with different particle sizes and surface treatments. *Polymer International, Vol. 55*, pp. 158-164.

Sun, C.C., Mark, J.E., (1989). Comparisons among the reinforcing effects provided by various silica based fillers in a siloxane elastomer. *Polymer, Vol. 30*, pp. 104-106.

Tavman, I. H., (1196). Thermal and Mechanical Properties of Aluminum Powder-Filled High-Density Polyethylene Composites. *Journal of Applied Polymer Science, Vol. 62*, pp.2161-2167 .

Tavman, I., Aydogdu, Y., Kök, M., Turgut, A., Ezan, A., (2011). Measurement of heat capacity and thermal conductivity of HDPE/Expanded graphite nanocomposites by differential scanning calorimetry. *Archives of Materials Science and Engineering, vol 50*, pp. 56-60.

Tanaka, T., (2005). Dielectric nanocomposites with insulating properties. *IEEE Transaction on Dielectric and Electrical Insulation, Vol. 12*, pp. 914-928.

Tekce, H. S., Kumlutas, D., Tavman, I. H., (2007). Effect of Particle Shape on Thermal Conductivity of Copper Reinforced Polymer composites. *Journal of Reinforced Plastics and Composites, vol. 26*, pp. 113-121.

Tian, M., Chen, G., Guo, S., (2005). Effect of high-energy vibromilling on interfacial interaction and mechanical properties of PVC/$CaCO_3$ composites. *Macromolecular Materials and Engineering, Vol. 290*, pp. 927-932.

Tibbetts, G.G., Lake, M.L., Strong, K.L. & Rice, B.P., (2007). A review of the fabrication and properties of vapor-grown carbon nanofiber/polymer composites. *Composite Science Technology, vol.67*, pp. 1709–1718.

Tu, H. & Ye, L., (2009). Thermal conductive PS/graphite composites. *Polymer Advanced Technology, vol.20*, pp. 21–27.

Veca, M.L., Meziani, M.J., Wang, W., Wang, X., Lu, F., Zhang, P., Lin, Y., Fee, R., Connell, J.W. & Sun, Y., (2009). Carbon nanosheets for polymeric nanocomposites with high thermal conductivity. *Advanced Material, vol. 21*, pp. 2088–2092.

Vlasveld, D.P.N., (2005). *Fibre reinforced polymer nanocomposites*, Technische Universiteit Delft. Thesis (PhD).

Wei, P.,Han, Z., Xu, X., Lı, Z., (2006). Synergistic flame retardent effect of SiO_2 in LLDPE/EVA/ATH Blends. *Journal of Fire Science, Vol. 24*, pp. 487-498.

Wong, Y.W., Lo, K.L. & Shin, F.G., (2001). Electrical and thermal properties of composite of liquid crystalline polymer filled with carbon black. *Journal of Applied Polymer Science, vol.82,* pp. 1549–1555.

Xıong, C., Lu, S., Wang, D., Dong, L., Jıang, D.D., Wang, Q., (2005). Microporous polyvinyl chloride: novel reactor for PVC/$CaCO_3$ nanocomposites. *Nanotechnology, Vol. 16,* pp. 1787-1792.

Yu, S., Hing, P. & Hu, X., (2002). Thermal conductivity of polystyrene–aluminum nitride composite. *Composites: Part A, vol.33*, pp. 289–292.

Zhang, X., Fujiwara, S. & Fujii, M., (2000). Measurements of thermal conductivity and electrical conductivity of a single carbon fiber. *International Journal of Thermophysics, vol.21*, pp. 965–980.

Zhou, H., Zhang, S. & Yang, M., (2007). The effect of heat-transfer passages on the effective thermal conductivity of high filler loading composite materials. *Composites Science and Technology, vol.67*, pp. 1035–1040.

Zuiderduın, W.C.J., Westzaan, C., Huetink, J., Gaymans, R.J., (2003). Toughening of polypropylene with calcium carbonate particles. *Polymers, Vol. 44*, pp. 261-275.